https://doi.org/10.71252/2177-34912025720038
ISSN: 2177-3491

Aerial imaging for early assessment of yield potential in maize[1]

Barbara Nascimento Santos[2*], *Nartênia Susane Costa Aragão*[2], *Mikaely Rosendo dos Santos*[3], *Tâmara Rebecca Albuquerque de Oliveira*[3], *José Jairo Florentino Cordeiro Junior*[3], *Gustavo Hugo Ferreira de Oliveira*[3]

[1] This article was derived from the undergraduate thesis of the first author and received no financial support.

[2] Universidade Federal de Sergipe, Programa de Pós-Graduação em Agricultura e Biodiversidade, São Cristóvão, Sergipe, Brazil. barbaranascimento2804@gmail.com; nartenia.aragao@gmail.com

[3] Universidade Federal de Sergipe, Departamento de Engenharia Agronômica do Sertão, Nossa Senhora da Glória, Sergipe, Brazil. mikaellyrosendodossantos285@gmail.com; tamara_rebecca@hotmail.com; jairofcordeiro@academico.ufs.br; gustavooliveira@academico.ufs.br

*Corresponding author: barbaranascimento2804@gmail.com

Editors:
Teogenes Senna Oliveira
Lucas Corrêdo

Submitted: June 06th, 2025.
Accepted: October 27th, 2025.

ABSTRACT

The use of unmanned aerial vehicles imagery has become an established practice in high-throughput phenotyping for predicting the yield potential of maize (*Zea mays* L.), although applying these technologies presents challenges due to regional specificities. This study aimed to assess the effectiveness of RGB (red, green, and blue) aerial imagery for the early identification of yield maize genotypes during the vegetative stage. Four genotypes were evaluated using a randomized block design with four replications. The experiment involved seven flights at two heights. Twenty-nine RGB vegetation indices were derived from image processing to discriminate genotypes based on plot-level grain yield. Nested models were fitted to predict temporal Best Linear Unbiased Predictions (BLUPs), with the most repeatable indices selected for analysis. Significant differences were observed among genotypes and plant spacing. The optimal flight timing was identified as 43 days after planting at a height of 80 meters. The indices MRCC, RmB, and RCC exhibited the highest repeatability and showed strong correlations with grain yield, demonstrating potential for RGB-based phenotyping studies. These findings highlight the utility of RGB imagery as a tool for early maize genotype selection, enhancing efficiency and accuracy in breeding programs and contributing to advancements in precision agriculture.

Keywords: High-throughput phenotyping, Plant breeding, unmanned aerial vehicles, *Zea mays* L.

This is an open access article distributed under the terms of the Creative Commons Attribution License (CC-BY), which permits unrestricted use, distribution, and reproduction in any medium, as long as the original work is properly cited.

INTRODUCTION

Maize (*Zea mays* L.) is one of the most widely cultivated cereals worldwide, playing a crucial role in global food security. Likely originating from Central America, this species exhibits remarkable versatility, contributing significantly to human and animal nutrition while also serving as a raw material for various industrial applications.[1,2] These factors enhance its economic value and drive continuous interest in its genetic improvement.

The increasing demand for higher productivity and climate resilience in maize production has intensified the need for precise and efficient genotype selection. In this context, high-throughput phenotyping (HTP) has emerged as a viable approach, facilitating applications ranging from plant localization and pest/disease detection to the identification of high-yielding genotypes in plant breeding programs.[3] Traditional phenotyping methods, while foundational, often present limitations in terms of efficiency, labor intensity, and accuracy, underscoring the necessity for advanced phenotyping technologies.

Unmanned Aerial Vehicles (UAVs) have gained prominence as a promising technological alternative for real-time, non-destructive crop monitoring. These platforms enable large-scale data acquisition across different growth stages, from early vegetative development to physiological grain maturity, offering valuable insights into plant performance under diverse environmental conditions.[4] UAV-based imaging techniques vegetation indices (VIs) derived from RGB, multispectral, and hyperspectral sensors to assess key agronomic traits, such as biomass accumulation, canopy architecture, and stress responses, which influence crop yield potential.[5,6]

Despite the potential of UAV-based phenotyping, several challenges hinder the standardization and scalability of these methodologies. Environmental variability, differences in UAV models, sensor types, and variations in flight parameters -such as altitude and image resolution- pose significant challenges to data consistency and comparability.[4,7,8] Furthermore, the effectiveness of these protocols is contingent upon optimized flight path planning, controlled image acquisition conditions, and robust data processing techniques to ensure reliable and reproducible results.

Most protocols described in the literature rely on multispectral or hyperspectral sensors, which, although highly accurate, are costly and often beyond the reach of many breeding programs in developing regions.[9-11] In contrast, RGB cameras represent a more affordable and readily accessible alternative. However, a significant research gap persists regarding the use of RGB imaging protocols for the early selection of maize genotypes before physiological maturity, particularly under semi-arid conditions in Brazil.

The development of a standardized RGB protocol adapted to these conditions represents a methodological innovation, since most previous studies have concentrated on multispectral and hyperspectral approaches, leaving cost-effective RGB applications underexplored in this context. Addressing this gap, the present study aims to establish an aerial phenotyping protocol utilizing RGB imagery to assess the yield potential of maize genotypes at early developmental stages, thereby enhancing the efficiency of selection processes in breeding programs.

MATERIALS AND METHODS

Experimental design and grain yield phenotyping

The field experiment was carried out in Nossa Senhora da Glória, Sergipe, Brazil (10°12'50.6" S, 37°19'03.2" W; with an altitude of 210 m), during the 2021 growing season. The predominant climate in the region is classified as type "tr**neb,[12]" with annual rainfall ranging from 506 to 1,301 mm. The soil at the experimental site is classified as an Argisol. Sowing was performed on May 22, 2021, and harvesting on November 13, 2021.

The experimental design employed was a Randomized Complete Block Design (RCBD) arranged in a strip plot scheme. The experiment was conducted with three different row spacings (0.60 m, 0.70 m, and 0.80 m) assigned to the strips, while the four maize genotypes were arranged within each strip, distributed across four replications.

Each plot consisted of two rows, each 8 m in length, with 0.20 m spacing between plants within rows, totaling 80 plants per plot, with one seed planted per hill. This arrangement corresponds to approximate plant densities of 83,333, 71,428, and 62,500 plants ha^{-1} for row spacings of 0.60 m, 0.70 m, and 0.80 m, respectively. The maize genotypes tested are described in Table 1.

UAV model and image acquisition

A drone model Mavic 2 Pro was used to conduct flights at heights of 60 and 80 meters, capturing RGB images (20 megapixels) with an 80% lateral and frontal overlap. Drone Deploy software (https://www.dronedeploy.com/)[13] was employed to plan and execute the flights. Five ground

control points (GCPs) were established at the vertices of the experimental area. Using GNSS RTK (FOIF model A60), coordinates were collected to prevent errors in the orthomosaics, which were georeferenced and generated after processing.

The flights were conducted between 11:00 AM and 1:00 PM, exclusively on sunny days, to minimize the influence of adverse weather conditions, such as cloud and precipitation, thereby ensuring the quality and consistency of the acquired images. A total of seven flights were performed at different heights on various dates (Figure 1), covering multiple phenological stages of the crop.

Image data processing

For image processing, the first step involved data mining of the images. This stage is crucial for the success of all subsequent analyses, as it encompasses image file segmentation, correction of potential errors, cropping of undesired areas, and other factors that influence the final purity of the image data.[6]

Therefore, to obtain the Orthomosaics, a flight plan was executed, delineating the experimental area to be surveyed during the crop season. Additionally, productivity data was collected through manual phenotyping (Figure 2-A). Subsequently, using the WebODM interface of the OpenDroneMap (ODM)[14] software on a 64-bit Windows plataform, image calibration took place to correct displacement errors utilizing control points, aiming to enhance the precision of the orthomosaic (Figure 2-B).

Table 1. Characterization of the genotypes used in the experiment implemented on 22/05/2021

Genotypes	Genetic class	Grain type	Technology	Company
1 GNZ16(EX3W07LVIP3)	SH	Semi-flint/ Orange	Vip3	GENEZE
2 GNZ59	SH	Semi-hard/ Orange	-	GENEZE
3 GNZ7720VIP3	SH	Semi-flint/ Orange	Vip3	GENEZE
4 AG8780	SH	hard	VTPRO3	AGROCERES

SH: Single-cross hybrids, VTPRO3: Vector triple protection 3, Vip3: Viptera 3. Source: Authors (2022)

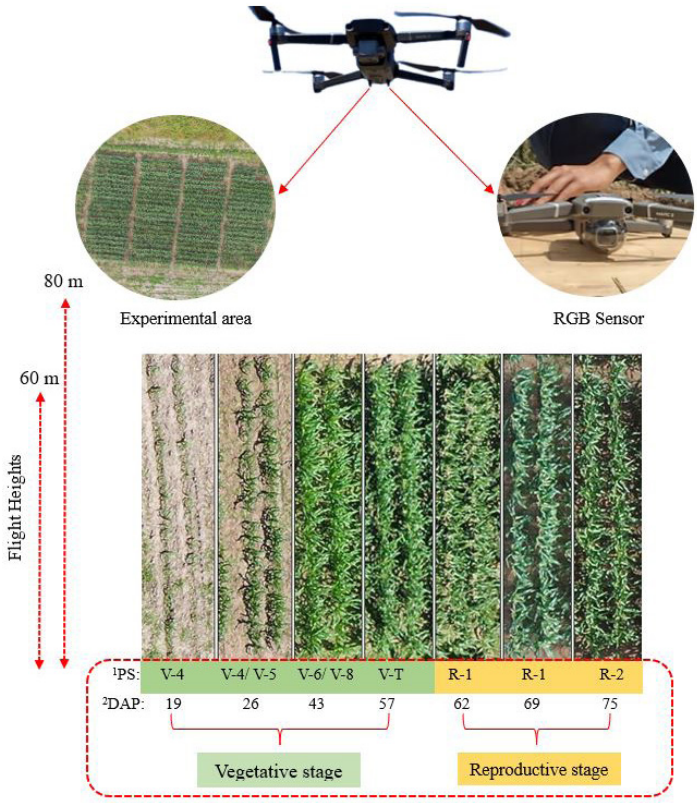

Figure 1. Image acquisition scheme using the Mavic 2 Pro drone at heights of 60 m and 80 m during different phenological stages of the crop. [1]PS: Phenological Stage, [2]DAP: Days after planting. Source: Authors (2022).

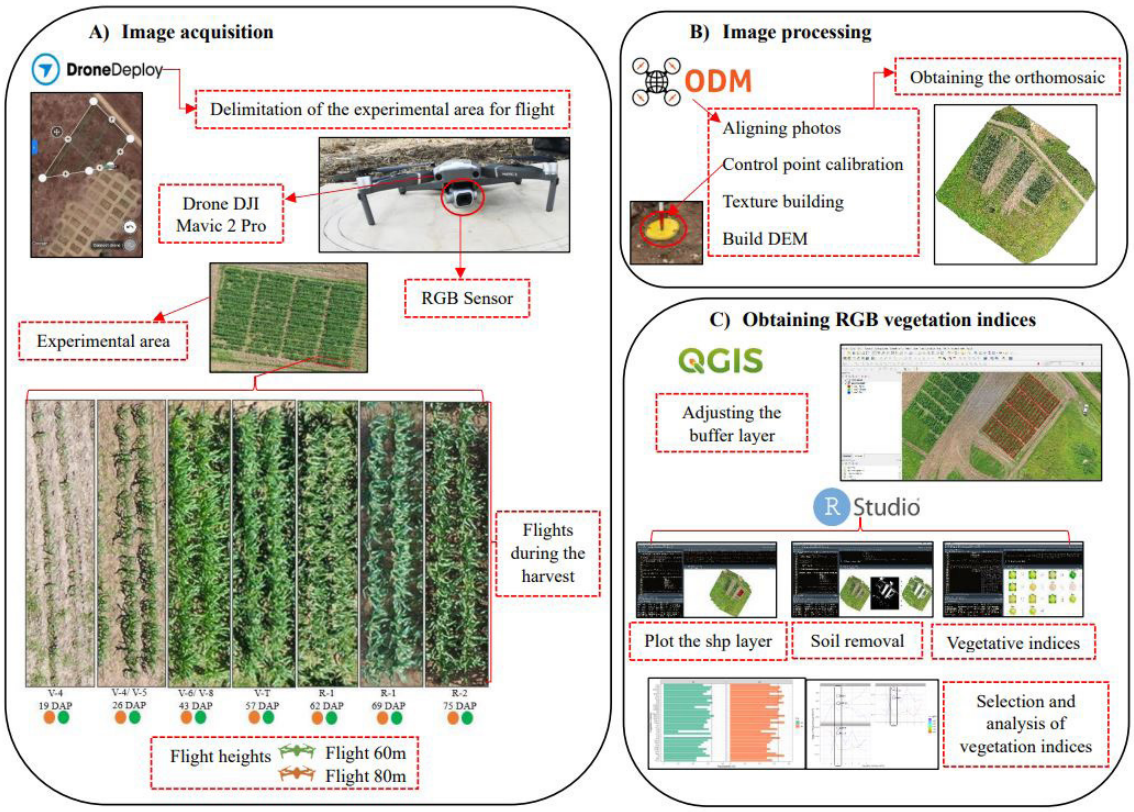

Figure 2. Workflow of the analyses conducted to obtain the 29 vegetation indices. Source: Authors (2022).

Image alignment was conducted with medium accuracy, employing 40,302 and 43,484 tie points, while the adaptive camera model adjustment was disabled. The mean reprojection error ranged from 1.35 to 1.47 pixels at flight heights of 60 m and 80 m, respectively. The adopted coordinate reference system was WGS 84 / UTM Zone 24S. The survey at 60 m height generated a Ground Sampling Distance (GSD) of 1.45 cm/pixel, whereas the 80 m flight resulted in a GSD of 1.94 cm/pixel. These resolutions were adequate for intra-plot variability analyses and for the extraction of spectral indices.

Finally, in the QGIS software, adjustments were made to the shapefile layer (shp) of the orthomosaic, including geometric correction, calibration, and border trimming, in order to improve spatial accuracy and image quality. These procedures facilitated the subsequent extraction of RGB vegetation indices in the RStudio software[15] (Figure 2-C).

A total of 29 vegetation indices (VIs) were extracted from the orthomosaics (Table 2). The selection of vegetation indices for the temporal BLUP analysis was grounded in their well-documented ability to detect changes in canopy structure, green vegetation, and biomass accumulation throughout the crop growth cycle.

To accomplish this, initially, a shapefile was created using the R function R/UAStools::plotshpcreate(). In the R software, polygons were generated around each plot for each genotype and row spacing based on the field map/sketch.

In the R software, the UAStools::plotshpcreate() function was used with the "buffer" argument set as "rowbuf = 0.1" and "rangebuf = 0.5" to delineate the plots, avoiding overlap of plants from adjacent plots. Since different spacings were used, the "rowespc = 0.8" function was employed, encompassing the widest row spacing used, facilitating the overlap of polygons in the plots. The shapefiles underwent preprocessing in the QGIS software[34] to adjust the polygons in each plot, minimizing errors in vegetation index extraction. At the end of the processing, 14 orthomosaics with adjusted shapefiles were obtained, seven for each flight altitude.

The FIELDimageR package was utilized in the R software for extracting the 29 VIs from each plot.[35] To achieve this, the RFIELDImageR::fieldMask function was used to eliminate soil color from the RGB images, with the HUE vegetation index serving this purpose. The fieldIndex function in R/FIELDImageR was employed to extract the

29 vegetation indices for each flight date. The VIs BI, GLI, NGRDI, VARI, and BGI were extracted using the "index=" argument, while the remaining indices were extracted through formulas using the "myIndex=" argument.

Statistical analysis for image phenotyping data

Conventional statistical analyses were conducted for the grain yield variable. Grain yield measurements were taken after harvesting the ears in each plot, weighed using a scale, and adjusted to 13% moisture content. An analysis of variance (equation 1) and a mean comparison test, specifically Tukey's test, were performed.

$$y_{ijk} = \mu + b_j + e_k + p_i + ep_{jk} + error(a)_{ik} + error(b)_{jk} + error(c)_{ijk} \quad (1)$$

In this model, y_{ijk} refers to the individual observation for each pedigree. The term μ denotes the overall mean of the response variable, expressed in kg/ha. The factor b_j represents the effect of the j^{th} block, while e_k refers to the effect of the k^{th} plant spacing. The pedigree (genotype) effect is represented by p_i, and the interaction between plant spacing and pedigree is expressed by $\$ep_{jk}$, which reflects how different genotypes respond to varying spacings. Additionally, three error terms are included: *error(a)*, representing the in-

Table 2. RGB Vegetation Indices applied in the phenotyping analyses

Vegetation indices	Equation[1]
Normalized green red difference index (NGRDI)[16]	(G-R)/G+R)
Green leaf index (GLI)[17]	(2*G-R-B)/(2*G+R+B)
Visible atmospherically resistant index (VARI)[18]	(G-R)/(G+R-B)
Spectral slope saturation index (SI)[19]	(R-B)/(R+B)
Blue green pigment index (BGI)[20]	B/G
Brightness index (BI)[21]	$\sqrt{R^2 + G^2 + B^2}/3$
Excess red (ExR)[22]	((1.4*R)-
Excess green minus excess red index (ExGR)[23]	((3*G)-(2.4*R)-B)
Excess green (ExG)[24]	((2*G)-R-B)
Normalized blue (BCC)[24]	B/(R+G+B)
Color index of vegetation extraction (CIVE)[25]	((0.441*R) (0.811*G)+(0.385*B)+18.78745)
Combined indices 1 (COM1)[26]	ExG + CIVE + ExGR+ VEG
Combined indices 2 (COM2)[27]	0.36*ExG + 0.47*CIVE + 0.17*VEG
Green minus red (GmR)[24]	G-R
Green minus blue (GmB)[24]	G-B
Green blue simple ratio index (GdB)[24]	G/B
Green red simple ratio index (GdR)[24]	G/R
Green chromatic index (GCC)[24]	(G/(R+G+B))
Modified excess green index (MExG)[28]	((1.262*G)-(0.884*R)-(0.311*B))
Modified green red vegetation index (MGVRI)[29]	((G^2)-(R^2))/((G^2)+(R^2))
Modified red chromatic coordinate index (MRCC)[4]	R^3/(R+G+B)
Normalized difference index (NDI)[23]	(G-R)/ (G+R)
Normalized difference red blue index (NDRBI)[30]	(R-B)/(R+B)
Normalized green-blue difference index (NGBDI)[31]	(GB)/(G + B)
Red minus blue index (RmB)[24]	R-B
Red blue simple ratio index (RdB)[24]	R/B
Red chromatic coordinate index (RCC)[24]	(R/(R+G+B)
Red green blue index (RGBVI)[29]	(((G^2)-(R*B))/((G^2)+(R*B)))
Triangular greenery index (TGI)[32]	(G-((0.39*R)-(0.69*B)))
Vegetative (VEG)[33]	G/R^0.667*B^0.334

[1] R= Red band; G= Green band; B= Blue band.

teraction between block and spacing; *error(b)*, referring to the interaction between block and genotype; and *error(c)*, representing the residual experimental error not explained by the previous components.

The statistical analyses of the temporally extracted vegetation indices, here referred to as Temporal Vegetative Indices (TVIs), as suggested by Adak et al. (2021),[4] and grain yield (GY) along with their graphical visualizations were conducted in the R software. To select the optimal post-planting flight date (PPD) for 60m and 80m altitudes and the most representative TVIs at each flight altitude, the repeatability index was employed.

For this purpose, nested mixed models were fitted to extract the BLUPs (Best Linear Unbiased Predictor) for each vegetation index for each pedigree. Considering them as a time series, they were termed as Temporal BLUPs (TBLUPs). The lmer4::lmer() function[36] was employed for this purpose.

The first fitted model is represented by equation 2, where the extraction of BLUPs for each vegetation index of each pedigree on each flight day was considered separately at 60m and 80m altitudes.

$$Y_{ijkl} = \mu + Pedigree_i + Spacing_k + Replication_j + Range_l + error_{ijkl} \quad (2)$$

Here, Y represents the individual observation of the vegetation index for each genotype. The term μ stands for the overall mean. *Pedigree* corresponds to the random effect of the ith genotype. The plant spacing (*Spacing*), replication (*Replication*), and field strip (*Range*) are all treated as random effects, each assumed to follow a normal distribution with mean zero and a specific variance. The residual term (*error*) captures the unexplained variation between the factors, also normally distributed.

The repeatability assessment of the vegetation indices was used as an indicator of the level of reproducibility as accuracy in choosing genotypes using sensors attached to Unmanned Aerial Vehicles (UAV). Therefore, repeatability values above 65% were considered high, as observed im previous studies by Herzig et al. (2021)[37] and Anderson et al. (2019),[38] which focused on evaluating the productivity of barley and corn, respectively.

The repeatability was calculated for each vegetation index, considering the variance explained by Pedigree and error, as represented by equation 3.

$$R = \frac{\sigma^2_{Pedigree(i)}}{\sigma^2_{Pedigree(i)} + \frac{\sigma^2_{error(ijkl)}}{j_{(jkl)}}} \quad (3)$$

Where $\sigma^2_{Pedigree}$ represents the variance attributed to the ith genotype, and σ^2_{error} corresponds to the residual variance, considering spacing, replication, and range. The term *j* refers to the number of replications.

In this study, the parameter estimated in Equation 3 was interpreted as repeatability (r), reflecting the consistency of vegetation index measurements across different replications and environments.

Although the model did not include the permanent environmental variance component typically incorporated in the formal definition of repeatability,[4] this component could not be estimated. In this context, the repeatability parameter is conceptually employed to represent the reliability and temporal stability of spectral measurements. High repeatability values (above 65%) indicate strong consistency in phenotyping and are essential for reliable genotype selection using UAV-based imaging data.

The second fitted model is represented by equation 4, where the extraction of Temporal BLUPs (TBLUPs) for the Temporal Vegetative Indices (TVIs) was considered for each pedigree at both 60 m and 80 m altitudes.

$$Y_{ijkl} = \mu + DAP_i + [Pedigree\,(DAP)]_{ij} + [Spacing\,(DAP)]_{im} + [Range\,(DAP)]_{ik} + [Replication\,(DAP)]_{il} + error_{ijkl} \quad (4)$$

The response variable Y corresponds to the vegetation index value for a given genotype at a specific time. The overall mean is denoted by μ and *DAP* is a fixed effect representing the flight date. All other terms, including genotype [*Pedigree*(*DAP*)], spacing [*Spacing*(*DAP*)], range [*Range*(*DAP*)], and replication [*Replication*(*DAP*)], are considered random effects nested within time, each assumed to follow a normal distribution. The residual error term captures the remaining unexplained variability.

The repeatability was calculated for each Temporal Vegetative Index (TVI), considering the variance explained by [Pedigree (DAP)]ij and error$_{ijkml}$, as represented by equation 5.

$$R_t = \frac{\sigma^2_{Pedigree(i,t)}}{\sigma^2_{Pedigree(i,t)} + \frac{\sigma^2_{error(ijklt)}}{j_{(jkl)}}} \quad (5)$$

In this expression, $\sigma^2_{Pedigree}$ denotes the variance explained by the ith genotype over time *t*, while σ^2_{error} represents the

residual variance associated with spacing, replication, range, and time. The term *j* corresponds to the number of replications. This measure evaluates the consistency of genotype performance over time and supports the identification of stable and high-performing genotypes across multiple flight dates.

Yield tracking with BLUPs over time

After selecting the VIs and TVIs that explained the highest proportion of variance among genotypes at different spacings estimated by repeatability, graphical representation was carried out to select the most representative flight altitude and track the temporal behavior of genotypes during the vegetative phase using the selected TVIs.

To track the productive performance of genotypes over time, the behavioral pattern of the selected TVIs was determined at each flight altitude. The BLUP of grain yield was used as a marker to distinguish genotypes above and below the average grain yield. For this purpose, the ggplot2::ggplot function[39] was employed. Next, Pearson's correlation analysis was applied to the BLUPs of grain yield and the selected vegetation indices to evaluate the strength and direction of their relationships. This analysis aimed to determine how effectively the spectral indices represented variations in yield.

RESULTS

Significant differences were observed among genotypes, indicating phenotypic variability grain yield, with coefficients of variation were within the acceptable range for the crop (Table 3). The genotypes GNZ59 and AG8780 exhibited the highest grain yields, with 5265.49 and 5275.95 kg/ha, respectively (Figure 3). These results are promising for maintaining genotypes with desirable traits in breeding programs, for use in future crosses.

It was observed that at 43 DAP, during the crop's vegetative stage, the vegetation indices exhibited significant repeatability for both tested flight heights (60m and 80m), as shown in Figure 4. Furthermore, in later growth stages, a decrease in repeatability was detected, suggesting that late-stage assessments using these indices are not effective for early selection.

Following the identification of the optimal period, the selection of VIs was conducted. For the flight at 60m height, the indices MRCC, RmB, and RCC exhibited the highest repeatability values, with 67.81%, 65.83%, and 65.39% at 43 DAP, respectively (Figure 5).

For the flight at 80 m height, the indices MRCC, Green, BI, Red, RmB, TGI, RCC, VARI, ExR, NDRBI, and MGVRI showed the highest repeatability values, with 73.91%, 73.69%, 73.25%, 73.17%, 72.37%, 70.33%, 70.23%, 68.04%, 67.38%, 67.01%, and 65.01% at 43 DAP, respectively, as illustrated in Figure 5. These results indicate that the mentioned indices are reliable for assessing genotype productivity during the vegetative stage.

The BLUPs obtained from vegetation indices selected based on the highest repeatability (as shown in Figure 5) demonstrated effectiveness in differentiating genotypes regarding grain yield at the determined flight point, at 43 DA (Figures 6 and 7).

Table 3. Summary of the analysis of variance for grain yield of the evaluated genotypes

SV	DF	MS
		GY
Block	3	162843
Spacing	2	3150949*
Error a	6	388435
Genotypes	3	3647216**
Error b	9	275649
Spacing x Genotypes	6	155818
Error c	18	100314
Residue	47	
Mean		5116.35
CV1 (%)		13.00
CV2 (%)		10.95
CV3 (%)		6.60

DF = Degrees of freedom; SV = Source of variation; CV = coefficient of variation; **, * Significance level at 1% and 5% probability by the F-test respectively; MS = Mean square, GY = Grain yield (kg/ha).

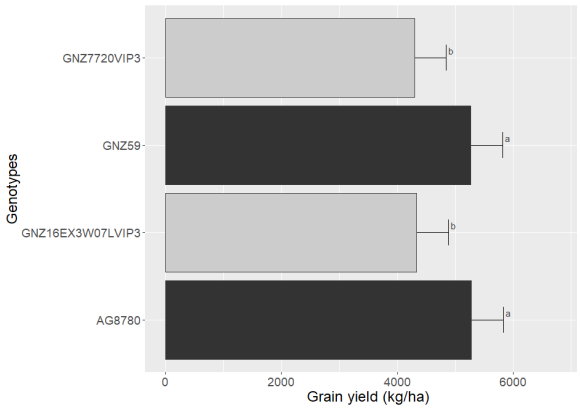

Figure 3. Tukey test for the grain yield of the genotypes evaluated. Bars with the same color and letters do not differ significantly.

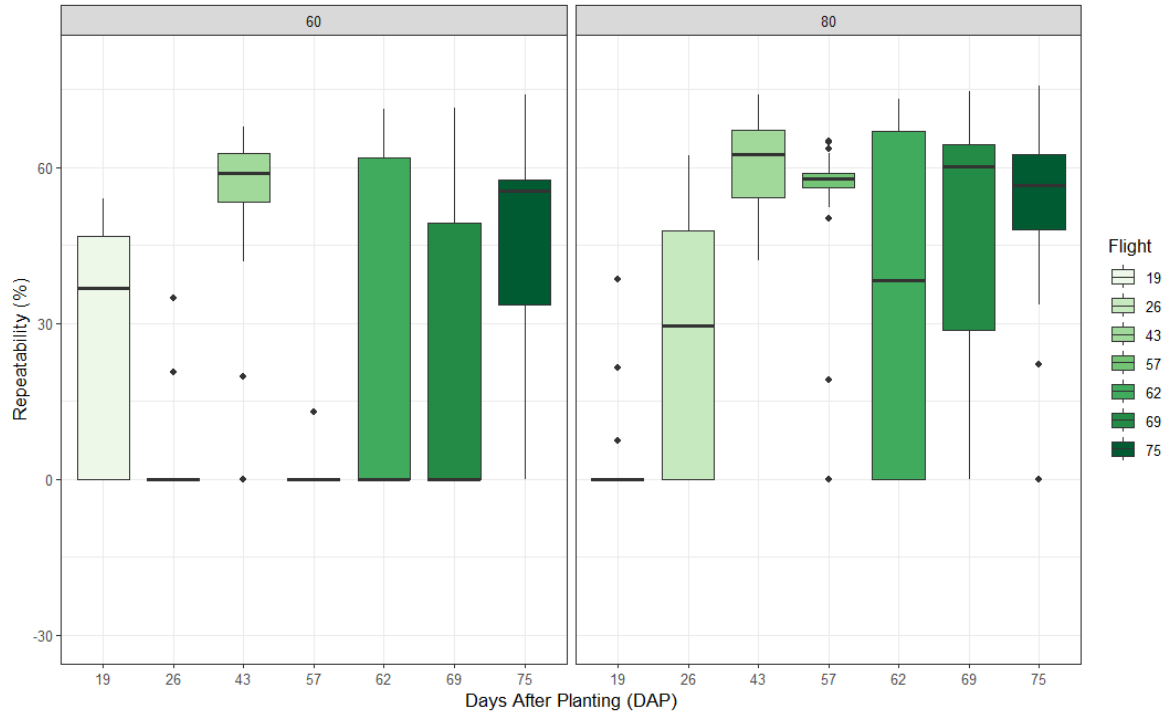

Figure 4. Identification of the best date of flight after planting using the repeatability of the RGB vegetation indices for the two flight heights evaluated.

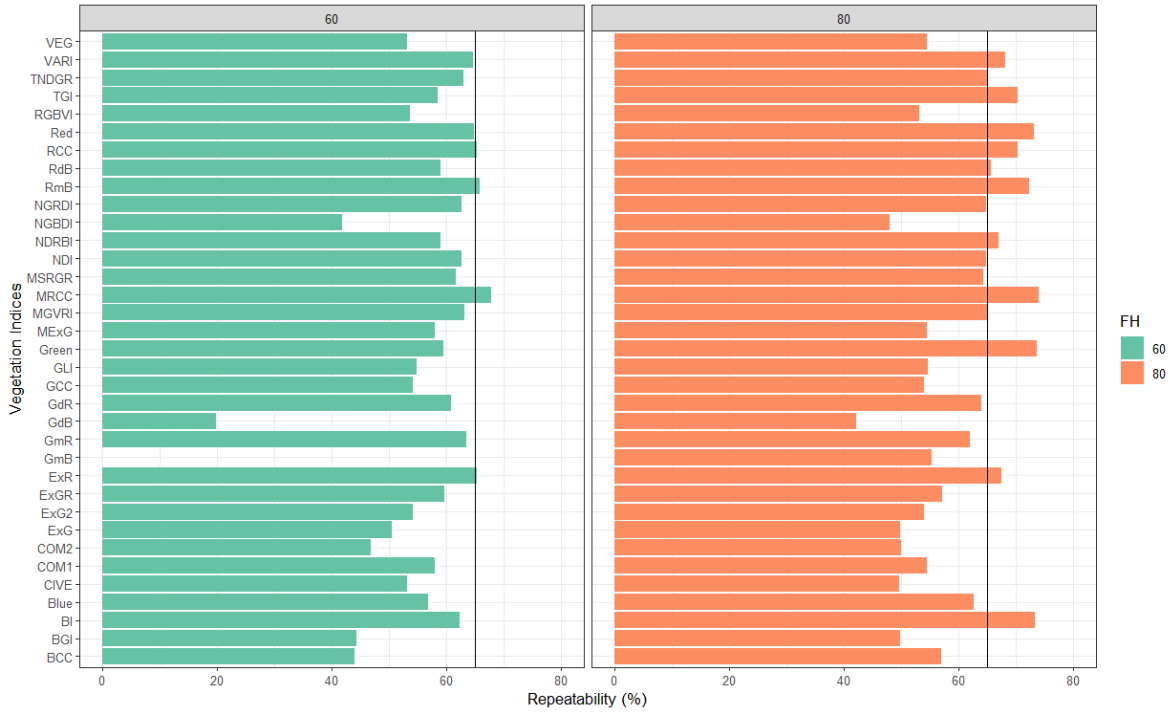

Figure 5. Identification of RGB Vegetation Indices with high repeatability at 60 and 80 meters height at 43 DAP. FH= Flight Height.

It is important to highlight in Figure 6 the behavior of the MRCC, RmB and RCC vegetation indices, which exhibited a relevant pattern for the research. The MRCC index showed the highest predicted values for the most productive genotypes, while the RmB and RCC indices displayed a consistent and similar behavior for high-yielding genotypes, indicating their potential for early detection of high-productivity genotypes.

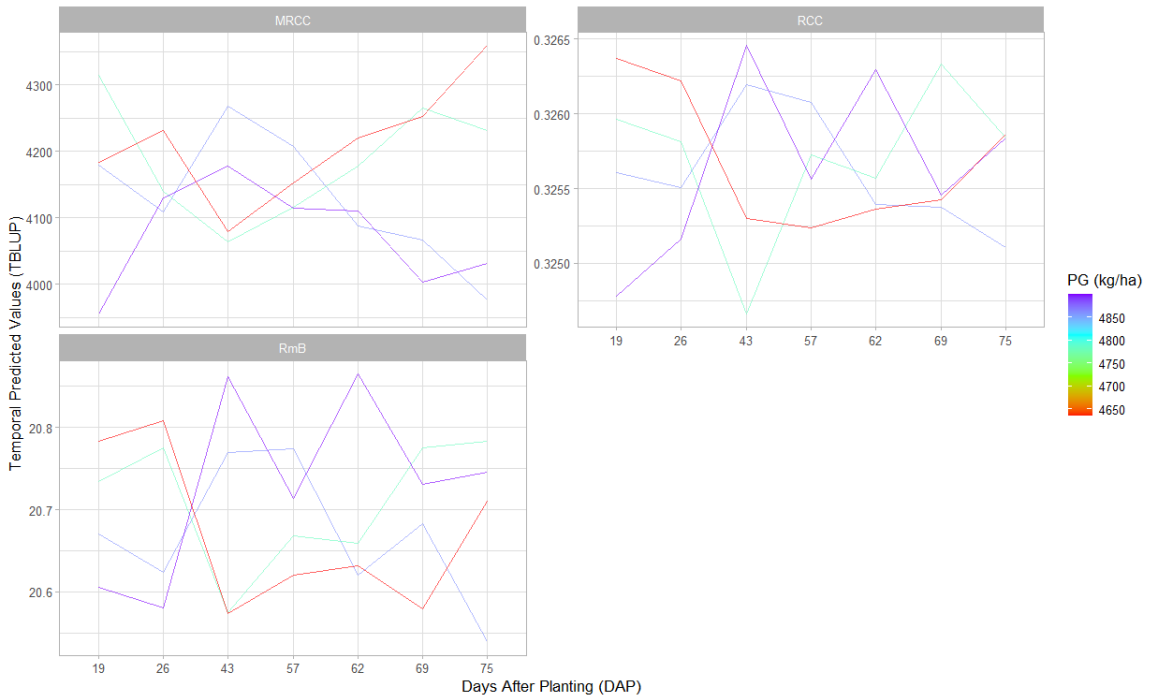

Figure 6. Line chart with temporal measurement with flight height at 60 meters, classified by grain yield per hectare.

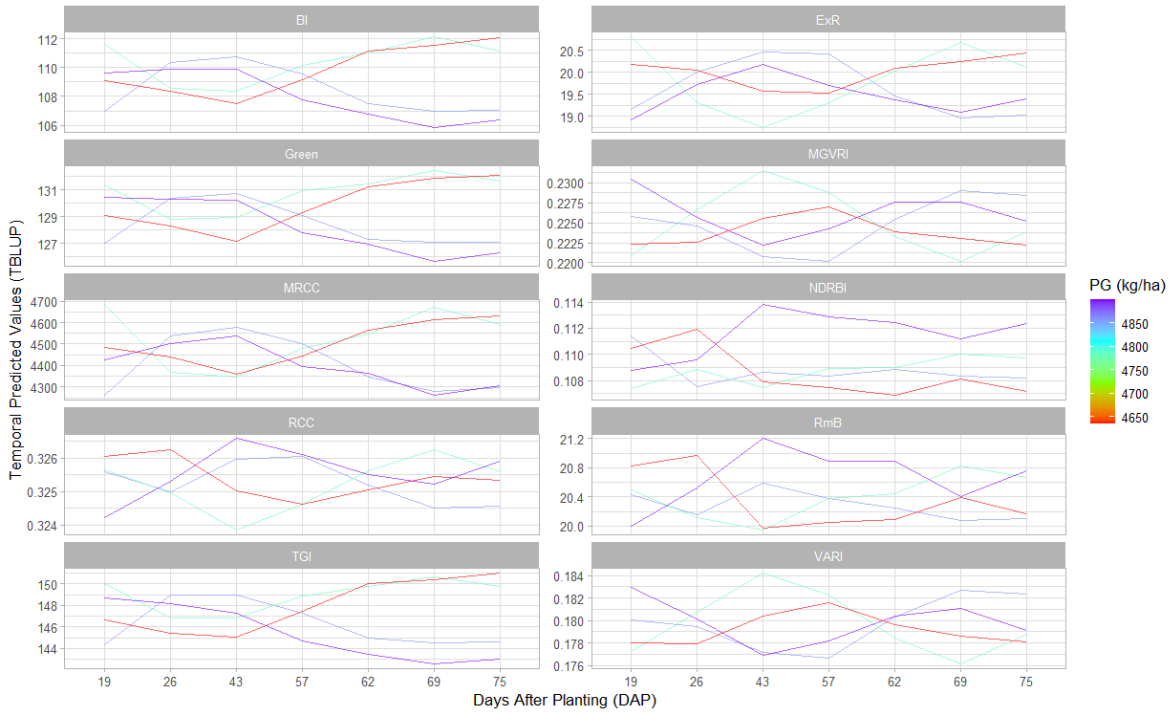

Figure 7. Line chart with temporal measurement with flight height at 80 meters, classified by grain yield per hectare.

Pearson's correlation analysis showed that the selected vegetation indices were strongly associated with grain yield (Tables 4 and 5).

At a flight height of 60 m, the MRCC, RmB, and RCC indices exhibited strong positive correlations with yield (r = 0.93–0.96), demonstrating their potential as reliable predictors of yield. Similarly, at 80 m, strong correlations were also observed (r = 0.88–0.99), confirming the consistency of these indices at different flight heights. These results highlight the effectiveness of the selected indices in representing the productive performance of the genotypes.

Table 4. Pearson correlation matrix between grain yield BLUPs and the selected vegetation indices at 43 DAP and a flight height of 60 m

PG	RCC	MRCC	RmB
1	0.93	0.93	0.96
0.93	1	0.83	0.94
0.93	0.83	1	0.78
0.96	0.94	0.78	1

Table 5. Pearson correlation matrix between grain yield BLUPs and the selected vegetation indices at 43 DAP and a flight height of 80 m

PG	RCC	MRCC	RmB
1	0.88	0.99	0.89
0.88	1	0.88	0.91
0.99	0.88	1	0.84
0.89	0.91	0.84	1

DISCUSSION

The findings of this study provide valuable insights into the early detection of maize genotypes with productive potential using RGB aerial images captured by unmanned aerial vehicles (UAVs). The phenotypic variability observed among the genotypes, reflected in significant differences in grain yield, highlights the effectiveness of high-throughput phenotyping (HTP) in enhancing selection processes within breeding programs.

Explanation of the most significant findings

The analysis of variance confirmed the phenotypic variability in grain yield among the evaluated genotypes, demonstrating excellent performance in the coefficient of variation, a parameter crucial for estimating the mean with reliability, as discussed by Gurgel et al. (2013).[40]

The high reproducibility of the MRCC, RmB and RCC vegetation indices underscores their accuracy in distinguishing maize genotypes during the vegetative phase. These indices are strongly associated with physiological attributes such as chlorophyll content, leaf area index, and photosynthetic efficiency, which are fundamental for biomass accumulation and, consequently, grain yield potential.[4,24]

The selection of the imaging period at 43 days after planting (DAP) aligns with key phenological stages (V6 to V8), characterized by rapid vegetative growth and canopy development.[41,42] This stage is crucial for establishing the potential number of grain rows, directly impacting yield outcomes.

The analyses of BLUPs derived from selected Vis proved to be satisfactory, demonstrating the ability to discern differences in the average productivity of genotypes at an early stage. This validation, as observed by Anderson et al. (2019),[38] highlights the potential of using images and Vis, even during the juvenile stage, for genotype selection.

These findings reinforce the reliability of employing aerial image phenotyping protocols for selecting maize genotypes in the juvenile stage using RGB images before the physiological maturity of the grain. These results have significant implications for maize breeding programs, expediting the prediction process of productive genotypes and ultimately reducing the time required to obtain these results.

Comparison with other studies

Our conclusions align with research by Anderson et al. (2019)[38] and Herzig et al. (2021),[37] which also confirmed the effectiveness of RGB indices in predicting the yield potential of maize and barley, respectively, achieving significant repeatability.

Resende et al. (2024)[43] demonstrated that RGB-derived indices, such as GLI and ExG, are strongly correlated with yield-related traits. In addition, the V5 and VT phenological stages were identified as the most appropriate periods for data collection. These results are in agreement with our findings, where indices obtained during early developmental stages exhibited greater discriminatory power. This reinforces the potential of RGB imagery for monitoring different phases of the crop cycle.

However, it is essential to consider the impact of environmental variability on the choice and applicability of vegetation indices. Thus, evaluating whether the study site accurately represents local growing conditions is crucial to ensure that the results are consistent with real production scenarios. The precision of the estimates relies not only on the selection of indices but also on the quality of the acquired images. In this context, flight altitude is a key parameter, as it directly influences spatial resolution.

In contrast to Maresma et al. (2020),[44] who reported optimal UAV flight heights around 100 meters, our study identified 80 meters as the most effective height for maize yield assessment.

Moreover, although authors such as Guo et al. (2023),[45] Abdulridha et al. (2023)[46] and Sahoo et al. (2024)[47] have

highlighted the superiority of hyperspectral and multispectral sensors, our findings suggest that RGB images, when processed with robust statistical models, can achieve equivalent predictive accuracy at a lower cost, particularly for early-stage phenotyping.

Practical implications and future directions

The identification of highly repeatable VIs such as MRCC, RmB, and RCC is particularly relevant for breeding programs, since their stability across flight dates and environments ensures greater reliability in early genotype selection.

This consistency allows breeders to make more confident decisions regarding genotype advancement at juvenile stages, thereby reducing the number of field trials. Furthermore, the operational simplicity and lower costs of RGB imagery compared to multispectral or hyperspectral approaches enhance its feasibility for large-scale use, especially in breeding programs with limited resources.

Nonetheless, it is important to recognize that the robustness of RGB indices does not necessarily eliminate the value of multispectral and hyperspectral sensors. In situations requiring fine discrimination of stress responses or nutrient status, broader spectral data may outperform RGB.

Future research should expand the scope to include a broader range of genotypes and environmental conditions to confirm the reliability of the identified indices. Comparative studies incorporating multispectral and hyperspectral data could further clarify the relative benefits of each image type.

CONCLUSION

This research highlights the effectiveness of RGB-based vegetation indices, particularly MRCC, RmB and RCC, in distinguishing early-stage maize genotypes. The practical guideline for UAV-based phenotyping protocols was identified at 43 DAP, with a flight height of 80 meters. Despite some limitations, these findings contribute to advancing high-throughput phenotyping methods, supporting more efficient breeding strategies and precision agriculture practices.

ACKNOWLEDGEMENTS. FINANCIAL SUPPORT AND FULL DISCLOSURE

The authors acknowledge the Federal University of Sergipe (UFS) and the Semi-Arid Plant Breeding Study Group (GEMS). This research received not any specific funding.

DATA AVAILABILITY STATEMENT

All datasets supporting the results of this study are available upon request from the corresponding author, Barbara Nascimento Santos.

AUTHOR CONTRIBUTIONS

Conceptualization: Barbara Nascimento Santos, Gustavo Hugo Ferreira de Oliveira.

Data acquisition: Barbara Nascimento Santos, José Jairo Florentino Cordeiro Junior, Mikaely Rosendo dos Santos, Nartênia Susane Costa Aragão, Tâmara Rebecca Albuquerque de Oliveira.

Data analysis: Barbara Nascimento Santos, Gustavo Hugo Ferreira de Oliveira, José Jairo Florentino Cordeiro Junior.

Design of methodology: Barbara Nascimento Santos, José Jairo Florentino Cordeiro Junior, Mikaely Rosendo dos Santos, Nartênia Susane Costa Aragão, Tâmara Rebecca Albuquerque de Oliveira.

Funding acquisition: Gustavo Hugo Ferreira de Oliveira.

Project administration: Gustavo Hugo Ferreira de Oliveira, José Jairo Florentino Cordeiro Junior, Tâmara Rebecca Albuquerque de Oliveira.

Writing and editing: Barbara Nascimento Santos, Gustavo Hugo Ferreira de Oliveira.

REFERENCES

1. Artuzo FD, Foguesatto CR, Machado JA, Oliveira L, Souza AR. O potencial produtivo brasileiro: uma análise histórica da produção de milho. Rev Agroneg Meio Ambient. 2019;12(2):515-40. doi: 10.17765/2176-9168.2019v12n2p515-540
2. Zhang H, Zhang R, Song Y, Miu X, Zhang Q, Qu J, et al. Enhanced enzymatic saccharification and ethanol production of corn stover via pretreatment with urea and steam explosion. Bioresour Technol. 2023;376:128856. doi: 10.1016/j.biortech.2023.128856
3. Danilevicz MF, Bayer PE, Boussaid F, Bennamoun M, Edwards D. Maize yield prediction at an early developmental stage using multispectral images and genotype data for preliminary hybrid selection. Remote Sens. 2021;13(19):3976. doi: 10.3390/rs13193976
4. Adak A, Murray SC, Božinovi´C S, Lindsey R, Nakasagga S, Chatterjee S, et al. Temporal vegetation indices and plant height from remotely sensed imagery can predict grain yield and flowering time breeding value in maize via machine learning regression. Remote Sens. 2021;13(11):2141. doi: 10.3390/rs13112141
5. Herr AW, Adak A, Carroll ME, Elango D, Kar S, Li C, et al. Unoccupied aerial systems imagery for phenotyping in cotton, maize, soybean, and wheat breeding. Crop Sci. 2023;63(4). doi: 10.1002/csc2.21028
6. Ampatzidis Y, Partel V, Costa L. Agroview: Cloud-based application to process, analyze and visualize UAV-collected data for precision agriculture applications utilizing artificial intelligence. Comput Electron in Agric. 2020;174:105457. doi: 10.1016/j.

compag.2020.105457

7. Wang W, Guo W, Le L, Yu J, Wu Y, Li D, et al. Integration of high-throughput phenotyping, GWAS, and predictive models reveals the genetic architecture of plant height in maize. Mol Plant. 2023;16(2):354-373. doi: 10.1016/j.molp.2022.11.016

8. Xiao J, Suab SA, Chen X, Singh CK, Singh D, Aggarwal AK, et al. Enhancing assessment of corn growth performance using unmanned aerial vehicles (UAVs) and deep learning. Measurement. 2023;214:112764. doi:10.1016/j.measurement.2023.112764

9. Zhang J, Dai L, Cheng F. Identification of corn seeds with different freezing damage degree based on hyperspectral reflectance imaging and deep learning method. Food Anal Methods. 2021;14(2):389-400. doi: 10.1016/j.compag.2021.106092

10. Abreu CA Júnior, Martins GD, Xavier LC, Bravo JV, Marques DJ, Oliveira GD. Defining the ideal phenological stage for estimating corn yield using multispectral images. Agronomy. 2023;13(9):2390. doi:10.3390/agronomy13092390

11. Bhargava A, Sachdeva A, Sharma K, Alsharif MH, Uthansakul P, Uthansakul M. Hyperspectral imaging and its applications: A review. Heliyon. 2024;10(12):e33208. doi:10.1016/j.heliyon.2024.e33208

12. Novais GT, Machado LA. Os climas do Brasil: segundo a classificação climática de Novais. Rev. Bras. Climatol. (Online). 2023;32:1-39. doi: 10.55761/abclima.v32i19.16163

13. DroneDeploy [Internet]. [S.l.]: DroneDeploy; [cited 2022 aug 21]. Available from: https://www.dronedeploy.com

14. OpenDroneMap/ODM GitHub Page; 2020 [cited 2022 mar 21]. Available from: https://github.com/OpenDroneMap/ODM

15. R Core Team. R: A language and environment for statistical computing. Version 4.2.1. R Foundation for Statistical Computing; 2022. Available from: https://www.R-project.org

16. Tucker CJ. Red and photographic infrared linear combinations for monitoring vegetation. Remote Sens Environ. 1979;8(2):127-150. doi: 10.1016/0034-4257(79)90013-0

17. Louhaichi M, Borman MM, Johnson DE. Spatially located platform and aerial photography for documentation of grazing impacts on wheat. Geocarto Int. 2001;16(1):65-70. doi: 10.1080/10106040108542184

18. Gitelson AA, Kaufman YJ, Stark R, Rundquist D. Novel algorithms for remote estimation of vegetation fraction. Remote Sens Environ. 2002;80(1):76-87. doi: 10.1016/S0034-4257(01)00289-9

19. Ceccato P, Flasse S, Tarantola S, Jacquemoud S, Grégoire JM. Detecting vegetation leaf water content using reflectance in the optical domain. Remote Sens environ. 2001;77(1):22-33. doi: 10.1016/S0034-4257(01)00191-2

20. Zarco-Tejada P, Berjon A, Lopezlozano R, Miller J, Martin P, Cachorro V, et al. Assessing vineyard condition with hyperspectral indices: Leaf and canopy reflectance simulation in a row-structured discontinuous canopy. Remote Sens Environ. 2005;99(3):271-287, 2005. doi: 10.1016/j.rse.2005.09.002

21. Richardson AJ, Wiegand CL. Distinguishing vegetation from soil background information. Photogramm. Eng Remote Sens. 1977; 43:1541–1552.

22. Meyer GE, Neto JC. Verification of color vegetation indices for automated crop imaging applications. Comput Electron Agric. 2008;63(2):282-293. doi: 10.1016/j.compag.2008.03.009

23. Meyer GE, Hindman TW, Laksmi K. Machine vision detection parameters for plant species identification. In G. E. Meyer & J. A. DeShazer (Eds.), Precision agriculture and biological quality. 1999. p. 327–335. (SPIE; vol. 3543).

24. Woebbecke DM, Meyer GE, Von Bargen K, Mortensen DA. Color indices for weed identification under various soil, residue, and lighting conditions. Trans ASAE. 1995;38(1):259-69. doi: 10.13031/2013.27838

25. Kataoka T, Kaneko T, Okamoto H, Hata S. Crop growth estimation system using machine vision. In: Proceedings 2003 IEEE/ASME International Conference on Advanced Intelligent Mechatronics (AIM 2003). IEEE; 2004. p. b1079-b1083 vol. 2. https://doi.org/10.1109/AIM.2003.1225492

26. Guijarro M, Pajares G, Riomoros I, Herrera PJ, Burgos-Artizzu XP, Ribeiro A. Automatic segmentation of relevant textures in agricultural images. Comput Electron Agric. 2011;75(1):75-83. doi: 10.1016/j.compag.2010.09.013

27. Guerrero JM, Pajares G, Montalvo M, Romeo J, Guijarro M. Support vector machines for crop/weeds identification in maize fields. Expert Syst Appl. 2012;39(12):11149-11155. doi: 10.1016/j.eswa.2012.03.040

28. Burgos-Artizzu XP, Ribeiro A, Guijarro M, Pajares G. Real-time image processing for crop/weed discrimination in maize fields. Comput Electron Agric.2011;75(2):337-346. doi: 10.1016/j.compag.2010.12.011

29. Bendig J, Yu K, Aasen H, Bolten A, Bennertz S, Broscheit J, et al. Combining UAV-based plant height from crop surface models, visible, and near infrared vegetation indices for biomass monitoring in barley. Int J Appl Earth Obs Geoinf. 2015;39:79-87. doi: 10.1016/j.jag.2015.02.012

30. Golzarian MR, Frick RA. Classification of images of wheat, ryegrass and brome grass species at early growth stages using principal component analysis. Plant Methods. 2011;7(1). doi: 10.1186/1746-4811-7-28

31. Hunt ER, Cavigelli M, Daughtry CS, Mcmurtrey JE, Walthall CL. Evaluation of digital photography from model aircraft for remote sensing of crop biomass and nitrogen status. Precis Agric. 2005;6:359-378. doi: 10.1007/s11119-005-2324-5

32. Hunt ER, Daughtry CS, Eitel JU, Long DS. Remote sensing leaf chlorophyll content using a visible band index. Agron J. 2011;103(4):1090-1099. doi: 10.2134/agronj2010.0395

33. Hague T, Tillett ND, Wheeler H. Automated crop and weed monitoring in widely spaced cereals. Precis Agric. 2006;7:21-32. doi: 10.1007/s11119-005-6787-1

34. QGIS [Internet]. [S.l.]: QGIS. Version 3.30.2; [cited 2022 Jun 22]. Available from: https://qgis.org

35. Matias FI, Caraza-Harter M, Endelman JB. FILDimageR. R package to analyze orthomosaic images from agricultural field trials. Plant Phenome J. 2020;3(1):20005. doi: org/10.1002/ppj2.20005

36. Bates D, Mächler M, Walker S. Fitting Linear Mixed-Effects Models Using lme4. J Stat Softw. 2014;67(1):1-48. doi: 10.18637/jss.v067.i01

37. Herzig P, Borrmann P, Knauer U, Klück HC, Kilias D, Seiffert U, Pillen K, Maurer A. Evaluation of RGB and Multispectral Unmanned Aerial Vehicle (UAV) Imagery for High-Throughput Phenotyping and Yield Prediction in Barley Breeding. Remote Sens. 2021;13(14):2670, 2021. doi: 10.3390/rs13142670

38. Anderson SL, Murray SC, Malambo L, Ratcliff C, Popescu S, Cope D, et al. Prediction of maize grain yield before maturity using improved temporal height estimates of unmanned aerial systems. Plant Phenome J. 2019;2(1):1-15. doi: 10.2135/tppj2019.02.0004

39. Wickham H. Ggplot2: Elegrant graphics for data analysis. Version 4.2.1. Springer, 2016. Available from: https://ggplot2.tidyverse.org

40. Gurgel FL, Ferreira DF, Soares AC. O coeficiente de variação como critério de avaliação em experimentos de milho e feijão. Belém, PA: Embrapa Amazônia Oriental-Boletim de Pesquisa e Desenvolvimento, 2013. p.80. Available from: http://www.infoteca.cnptia.embrapa.br/infoteca/handle/doc/955896

41. Magalhaes PC, Durães FO. Fisiologia da produção de milho. Sete Lagoas: Embrapa Milho e Sorgo; 2006. (Circular Técnica, 76). Available from: https://ainfo.cnptia.embrapa.br/digital/bitstream/CNPMS/19620/1/Circ_76.pdf

42. Viana LA, Zambolim L, Sousa TV, Tomaz DC. Potential use of thermal camera coupled in UAV for culture monitoring. Braz J Biosyst Eng. 2018;12(3):286-298. doi: 10.18011/bioeng2018v12n3p286-298

43. Resende EL, Bruzi AT, Cardoso ED, Carneiro VQ, Souza VA, Barros PH, Pereira RR. High-throughput phenotyping: application in maize breeding. AgriEngineering. 2024;6(2):1078-92. doi:10.3390/agriengineering6020062

44. Maresma A, Chamberlain L, Tagarakis A, Kharel T, Godwin G, Czymmek KJ, et al. Accuracy of NDVI-derived corn yield predictions is impacted by time of sensing. Comput Electron Agric. 2020;169:105236. doi: 10.1016/j.compag.2020.105236

45. Guo Y, Xiao Y, Hao F, Zhang X, Chen J, Beurs K, et al. Comparison of different machine learning algorithms for predicting maize grain yield using UAV-based hyperspectral images. Int J of Appl Earth Obs Geoinf. 2023;124:103528. doi: 10.1016/j.jag.2023.103528

46. Abdulridha J, Min A, Rouse MN, Kianian S, Isler V, Yang C. Evaluation of stem rust disease in wheat fields by drone hyperspectral imaging. Sensors. 2023;2398):4154. doi: 10.3390/s23084154

47. Sahoo RN, Rejith RG, Gakhar S, Ranjan R, Meena MC, Dey A, et al. Drone remote sensing of wheat N using hyperspectral sensor and machine learning. Precis Agric. 2024;25(2):704-728. doi: 10.1007/s11119-023-10089-7